Available online at www.sciencedirect.com

ScienceDirect

Ceramics International 34 (2008) 1773–1778

CERAMICS INTERNATIONAL

www.elsevier.com/locate/ceramint

Characteristics of YSZ synthesized with a glycine-nitrate process

Qigen Wang [a], Ranran Peng [a], Changrong Xia [a,*], Wei Zhu [a,b], Huanting Wang [b]

[a] *Laboratory for Renewable Clean Energy, Department of Materials Science and Engineering,*
University of Science and Technology of China, Hefei, Anhui 230026, China
[b] *Department of Chemical Engineering, Monash University, Clayton, Vic. 3800, Australia*

Received 18 September 2006; received in revised form 1 May 2007; accepted 12 June 2007

Abstract

The amount of glycine addition was optimized for synthesizing $(Y_2O_3)_{0.08}(ZrO_2)_{0.92}$ (YSZ) powders with a glycine-nitrate process. The effect of glycine quantity was investigated on the phase structure, sintering behavior, electrical performance and microstructure of the resulted YSZ powders. With the increase of glycine addition, the crystallite size of the YSZ powder increased, the specific surface area decreased, and the density of the sintered YSZ pellets decreased when they were fired at the same temperature. Thermodynamic calculation showed that the flame temperature of the glycine-nitrate combustion reaction was much higher when more glycine was used. A highly loose powder was thus obtained with low quantity of glycine addition. When 70% of stoichiometric amount of glycine was used, YSZ powder had the highest densification rate. AC impedance spectroscopy showed that the amount of glycine had effects not only on total conductivity, but also on grain boundary and bulk contributions. The highest conductivity attained a value of 0.027 S cm^{-1} at 800 °C for YSZ prepared with 80% of stoichiometric amount of glycine.

Keywords: Yttria-stabilized zirconia; Glycine-nitrate process; Synthesis; SOFC

1. Introduction

Among the phases of doped zirconia the cubic phase has the highest electrical conductivity [1]. The cubic phase $(Y_2O_3)_{0.08}(ZrO_2)_{0.92}$, 8YSZ is widely used as electrolyte materials in solid oxide fuel cells (SOFC), oxygen sensors, oxygen separation membranes, and oxygen pumps as it has high ionic conductivity, good mechanical strength, and chemical stability at high temperature [2–5]. The ionic conductivity of the YSZ electrolyte is related not only to dopant concentration, but also to processing technology of the powders, particle sizes, and sintered density, etc. Gibson et al. [5] has studied the relationship between sintered density and its ionic conductivity, showing that sintered density is not the only factor affecting conductivity. The other important factor is the powder characteristics. Traditionally, dry powder processing consists of mixing zirconia powder or zirconium oxychloride with a stabilizing agent (oxides, nitrates, carbonates, etc., of bi- and tri-valent cations) and heating the mixture for several hours, to produce non-stoichiometric solid oxide solutions, which usually yields large particle size, in homogeneity and poor reactivity, leading to a higher sintering temperature. To improve the powder sintering activity and reduce the temperature for cubic phase formation, methods such as sol–gel, precipitation, and hydrothermal routes were employed to prepare YSZ powders [1,6–8]. Usually, the powder characteristic depends on the fabrication methods. The cubic phase YSZ produced at low temperatures by wet methods may contain some residual –OH or water that affect the sinterability. Therefore, the effects of preparation parameter and powder firing temperature on the powder characteristics are crucial to optimize the properties of the YSZ electrolyte. The glycine-nitrate process (GNP), which possesses the characteristics of a wet chemical route, is a self-sustained combustion technology for the preparation of ultra-fine powders. This method does not require special igniting equipment, and the igniting temperature is lower, and the operation is simple and easy as well. In addition, this process can result in highly porous form-like powders, which can be used to prepare dense ceramic films with a cost-effective dry-press technique [9,10]. Using the GNP process, solid solutions

---

* Corresponding author. Tel.: +86 551 3607475; fax: +86 551 3606689.
E-mail address: xiacr@ustc.edu.cn (C. Xia).

0272-8842/$34.00 © 2007 Elsevier Ltd and Techna Group S.r.l. All rights reserved.
doi:10.1016/j.ceramint.2007.06.003

such as $Ce_{0.9}Gd_{0.1}O_{1.95}$, $La_{0.8}Sr_{0.2}MnO_3$ and 8YSZ with improved performances have been prepared [11–13]. He et al. [13] have prepared YSZ powders with the GNP process using $ZrOCl_2{\cdot}8H_2O$, Y_2O_3, glycine and HNO_3 as starting materials. A comparative study was carried out to evaluate the effects of 1:1 M and 1:2 M ratio of metal ions/glycine (denoted as *M*/*G*) and heat-treatment temperature (fired at 1000 °C and 1200 °C) on the property of YSZ powders. It was reported that the optimal electrical property of YSZ electrolyte could be obtained after pre-heating at 1000 °C for 6 h and finally sintering at 1450 °C for 6 h when an *M*/*G* ratio of 1:2 was adopted, and the conductivity attained a value of 0.024 S cm^{-1} at 800 °C. In this work, highly porous nano-sized YSZ powders were synthesized with the GNP process. The optimized powder was used for preparing dense YSZ films with the dry-press technique. This study emphasizes the effects of different amount of glycine on the properties of the derived YSZ powders.

2. Experiment

2.1. YSZ powder preparation

$Zr(NO_3)_4{\cdot}5H_2O$ (99.9%), $Y(NO_3)_3{\cdot}6H_2O$ (99.9%), and NH_2CH_2COOH (99.9%) were used as starting materials and dissolved in distilled water to form a solution in which Zr^{4+} and Y^{3+}concentrations meet the formula of $(Y_2O_3)_{0.08}(ZrO_2)_{0.92}$. The solution was stirred for 1 h and then heated on a hot plate under stirring. It was converted to a viscous gel due to evaporation, and ignited to flame. The self-sustained combustion resulted in fine YSZ ash of pale-grey in color. The ash was subsequently fired at temperature from 600 °C to 1200 °C for 2 h to remove possible carbon residues and to form a well-crystallized YSZ. The amount of glycine for the formation of YSZ can be calculated according to the following equations:

$$\begin{aligned}&9Zr(NO_3)_4 + 20NH_2CH_2COOH\\&\quad = 9ZrO_2 + 28N_2 + 50H_2O + 40CO_2\end{aligned} \tag{1}$$

$$\begin{aligned}&6Y(NO_3)_3 + 10NH_2CH_2COOH\\&\quad = 3Y_2O_3 + 14N_2 + 25H_2O + 20CO_2\end{aligned} \tag{2}$$

Therefore, 1 mol YSZ stoichiometrically requires 2.31 mol glycine. To investigate the effect of glycine quantity on YSZ characteristics, glycine addition was set from 70% to 120% of the stoichiometric amount. The resulted YSZ powder was termed as 70-YSZ, 80-YSZ, 90-YSZ, 100-YSZ, 110-YSZ, and 120-YSZ, respectively. For example, 70-YSZ means the YSZ powder was prepared using 2.31 × 70% = 1.617 mol glycine/mol YSZ.

2.2. Powder characterization

Phase identification was performed using powder X-ray diffraction (D/Max-γA, Japan) with Cu Kα (λ =1.5418 Å) and a scanning range of 20–80°. Average crystallite sizes were estimated using the scherrer equation $D_{XRD} = k\lambda/\beta\cos\theta$ ($k = 0.89$) [13]. The powders were uniaxially pressed under 200 MPa to form pellets of 13 mm in diameter and about 1 mm in thickness. The green pellets were then sintered at 1400 °C for 5 h with a heating rate 3 °C/min. Linear shrinkage of the green pellet was measured in air using a dilatometer (Netzsch, DIL402C), at a heating rate of 10 °C/min. Density was measured according to the Archimedes principle. Specific surface area of the powders was measured with isothermal nitrogen adsorption–desorption technique. Average particle size (D_{BET}) was estimated with the specific surface area (S_{BET}) according to $D_{BET} = 6/\rho S_{BET}$ where ρ is 5.959 g/cm^3, the theoretical density of YSZ (PDF#30-1468). A scanning electron microscope (JSM-6700F, JEOL) was used to detect the microstructure of the sintered pellets and powder morphology. Conductivity was determined using AC impedance measurement with frequency range from 0.1 Hz to 100 kHz. Before measurements, silver electrodes were prepared by deposition of silver paste onto both sides of the pellets. The conductivity, σ, can be calculated with $\sigma = L/RA$, where L is the thickness of the sample, A the electrode area, and R is the resistance as determined with the impedance spectroscopy.

3. Results and discussion

3.1. Powder characteristic

The X-ray powder diffraction pattern showed that heating the ash at temperature above 600 °C resulted in a cubic YSZ powder. The XRD peaks were rather broad at 600 °C. Consequently it was difficult to distinguish between cubic and tetragonal structures at this temperature. Increasing the fire temperature, a simultaneous growing and narrowing of the peaks were observed due to better crystallization and enhanced crystallite size. Shown in Fig. 1 is the average crystallite size estimated using the Scherrer formula with (3 1 1) peak. The crystallite size increases with the firing temperature very slowly up to 1000 °C. Rapid growth was observed at temperature above 1000 °C from 25 nm at 1000 °C to 78 nm at 1100 °C.

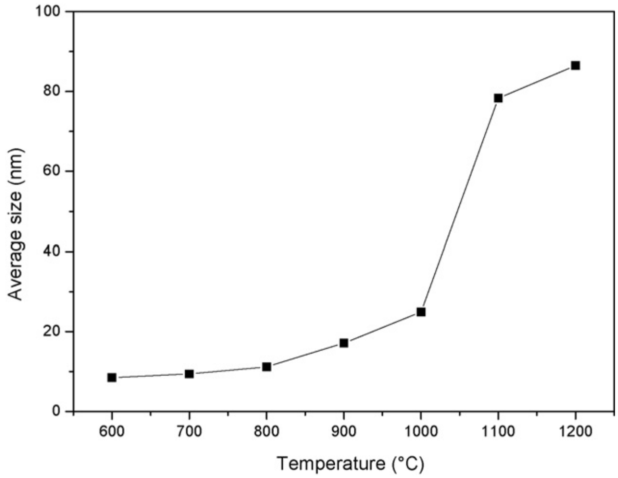

Fig. 1. Effect of the firing temperature on the crystalline size of 80-YSZ powder.

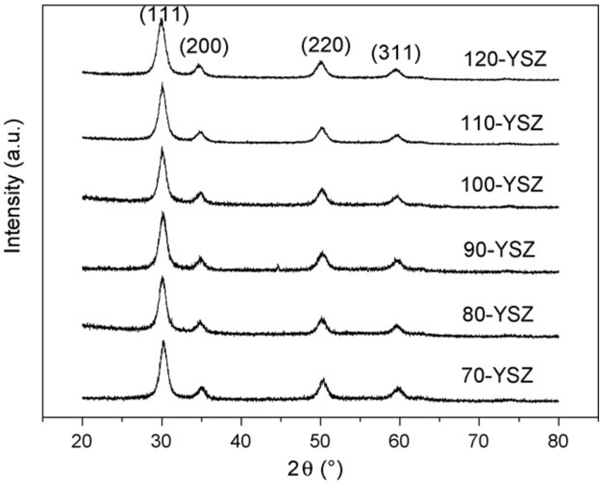

Fig. 2. XRD pattern of YSZ powers prepared with different amount of glycine and fired at 700 °C.

Shown in Fig. 2 are XRD pattern for powders prepared with different amount of glycine and fired at 700 °C for 2 h. As shown in Fig. 2, all the powders fired at 700 °C exhibited a cubic phase, which was not affected by the amount of glycine addition. As the glycine amount increased, the width of the diffraction peaks decreased, indicating the increase in crystallite size. The relation between the amount of glycine and crystallite size, D_{XRD}, is shown in Table 1. The crystallite size increases readily from 8.0 nm when 70% of stoichoimetric glycine was used to 16 nm as a result of stoichoimetric reaction, further to 34 nm when 120% glycine was added.

The specific surface areas are also summarized in Table 1. The areas decreased with the amount of glycine addition. Average particle size, D_{BET}, which was estimated from the specific surface area with the assumption that the powder consisted of dense and spherical particles, increased with the glycine quantity. This is consistent with the crystallite size estimated with XRD. However, D_{XRD} is smaller than D_{BET}. The cubic phase YSZ, which was produced with wet methods, may contain some residual facial –OH and adsorb H_2O producing surface energy that impel grains to form agglomerates. This might be the reason for $D_{\mathrm{XRD}} < D_{\mathrm{BET}}$. Further, considering the fact that $D_{\mathrm{BET}}(70\%)/D_{\mathrm{XRD}}(70\%) = 8.7$, and $D_{\mathrm{BET}}(120\%)/D_{\mathrm{XRD}}(120\%) = 3.9$, one could deduce that as the amount of glycine increases, the agglomeration degree of single grains decreases. This suggests that the facial residual –OH and H_2O decrease with the amount of glycine. A high –OH and H_2O residual loading generally means high surface energy and thus high degree of agglomeration. So with the increase of glycine quantity, the agglomeration degree decreased and consequently, the loading of residual –OH and H_2O reduced.

The glycine quantity will affect the glycine-nitrate combustion reaction, which is a heat release process. The highest flame temperature can be thermaldynamically estimated under the assumption that the combustion is an adiabatic process. This assumption is made based on the fact that the combustion completes in a very short time. If the flame temperature is T for the stoichiometric combustion, the temperature for the non-stoichiometried reaction can be estimated. The result is shown in Table 1. The more glycine was used, the higher the temperature. High temperature leads to further crystalline growth, thus high D_{XRD} and low S_{BET}. Low –OH and H_2O residual loading also associated with high temperature, thus low degree of agglomeration.

The morphology of YSZ particle was also affected by the glycine quantity. Shown in Fig. 3 are the microstructure views of YSZ powder prepared with different amount of glycine. When 70% glycine was used, porous and highly loose particles with a foam-like morphology were observed. The loose and porous structures as shown in Fig. 3(a) seem to result from the great amount of gases released by the redox reaction [14]. Increase of glycine quantity resulted in less porous particles as shown in Fig. 3(b) and (c). The loose particles show very low packing density. It is only 0.35% of the theoretical density for 70-YSZ particles, when no pressure is applied to the packing body. Such low particle density makes it possible to prepare dense YSZ film less than 10 μm with a dry-press technique, however using commercial micro-size YSZ is very difficult to press a film thinner than 50 μm by the traditional dry pressing method [15].

3.2. Sintering and densification of samples

Shown in Fig. 4(a) are dynamic sintering curves of the green compacts prepared with powders synthesized using different amount of glycine and fired at 700 °C. It can be seen that an obvious increase of the linear shrinkage begins at 1100 °C for the 70-YSZ. The shrinkage of the 70-YSZ compact is highest. Shown in Fig. 4(b) are the corresponding $d(dL/L_0)/dT$ curves. There is only one shrinkage peak for the 70-YSZ compact. The peak corresponds to 1300 °C indicating the highest densification rate. The other two curves have two peaks. The highest densification rate occurred at temperature above 1400 °C.

Table 1
Characteristics of YSZ powders synthesized with different amount of glycine and fired at 700 °C for 2 h

Glycine quantity	70%	80%	90%	100%	110%	120%
D_{XRD} (nm)	8.0	9.4	9.8	16	23	34
S_{BET} ($m^2\,g^{-1}$)	14.44	13.47	12.93	9.54	9.08	7.56
D_{BET} (nm)	69.8	74.9	78.0	106	111	134
$D_{\mathrm{BET}}/D_{\mathrm{XRD}}$	8.7	8.0	7.9	6.6	4.9	3.9
Estimated flame temperature (K)	$T - 423$	$T - 250$	$T - 85$	T	$T + 81$	$T + 103$
Conductivity at 800 °C (S/cm)	0.024	0.027	0.018	0.018	0.018	0.020

The estimated flame temperature and measured conductivity at 800 °C are also listed.

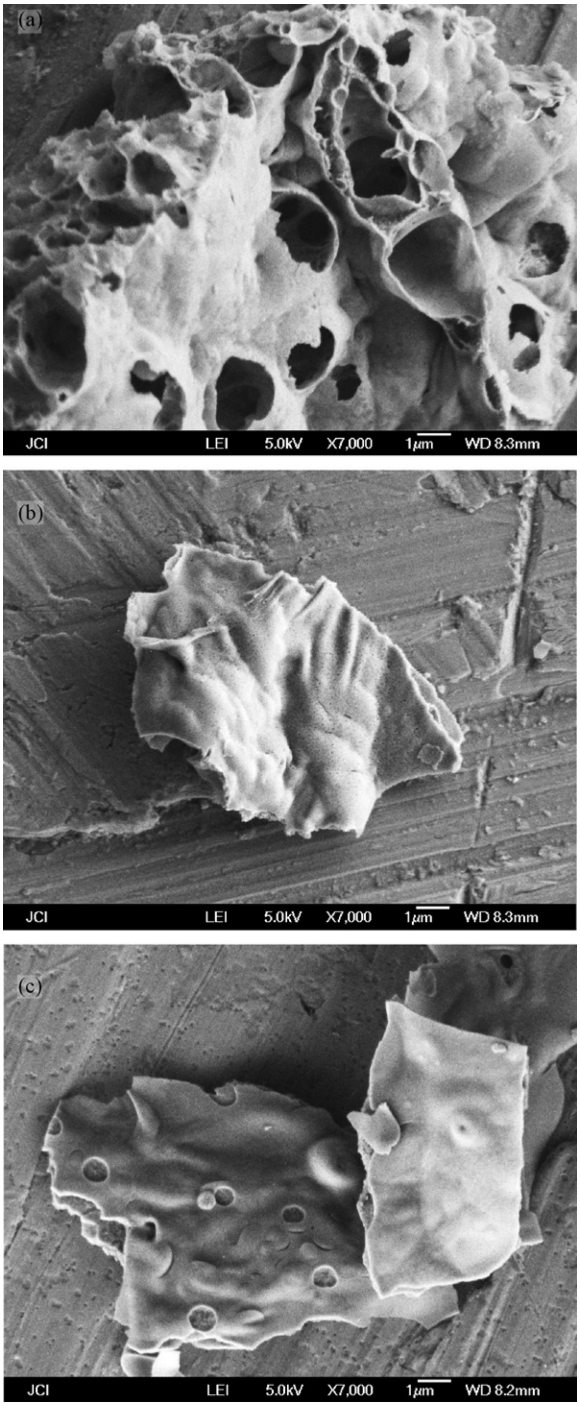

Fig. 3. SEM photographs of YSZ powders heated at 700 °C. (a) 70-YSZ, (b) 100-YSZ, and (c) 120-YSZ.

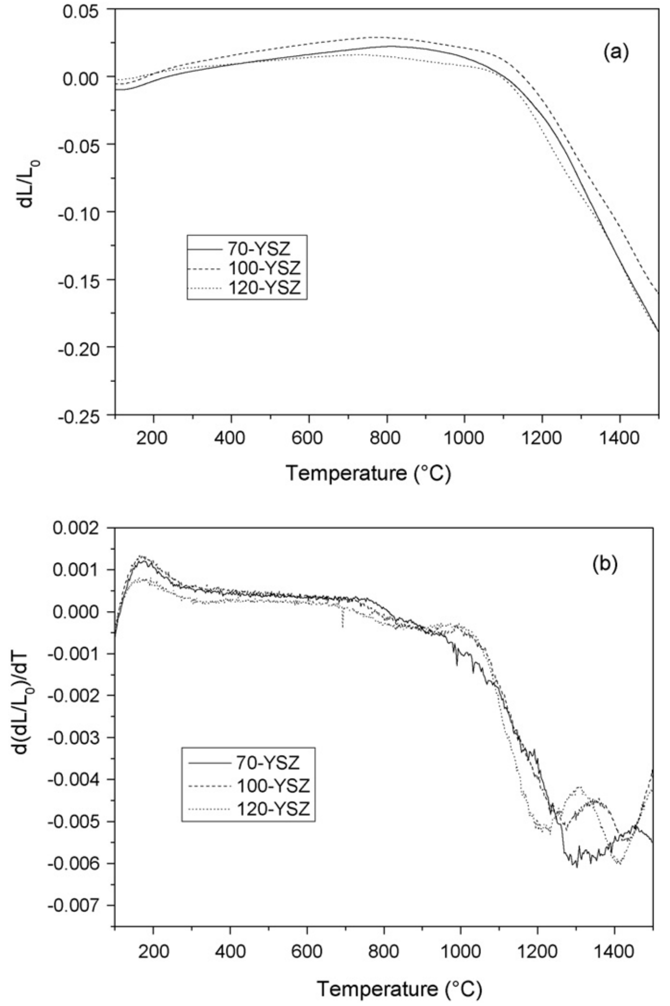

Fig. 4. Linear shrinkage curves (a) and their derivations (b) for green YSZ compacts.

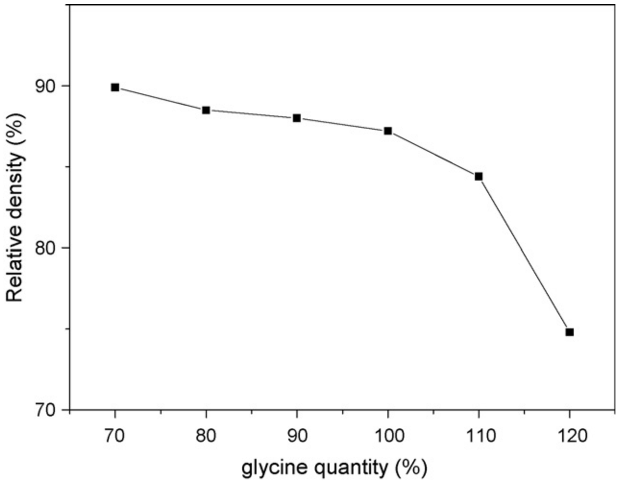

Fig. 5. Relative density of YSZ pellets prepared with different amount of glycine addition and sintered at 1400 °C for 5 h.

These inferred that 70-YSZcompact is much easier to be densified than the other samples.

The effect of glycine quantity on YSZ sinterability was further investigated by measuring the pellet density. Shown in Fig. 5 is the relative density for pellets sintered at 1400 °C for 5 h and fabricated with different amount of glycine addition. The relative density decreased, when more glycine was used. For the 70-YSZ sample, density up to 90% of the theoretical value was reached. It decreased to 75% for the 120%-YSZsample. This meets with the result of linear shrinkage measurement. The lower density derived by higher amount of glycine might be due to the reason that more glycine caused coarser particles, which are generally harder to be densified than fine particles.

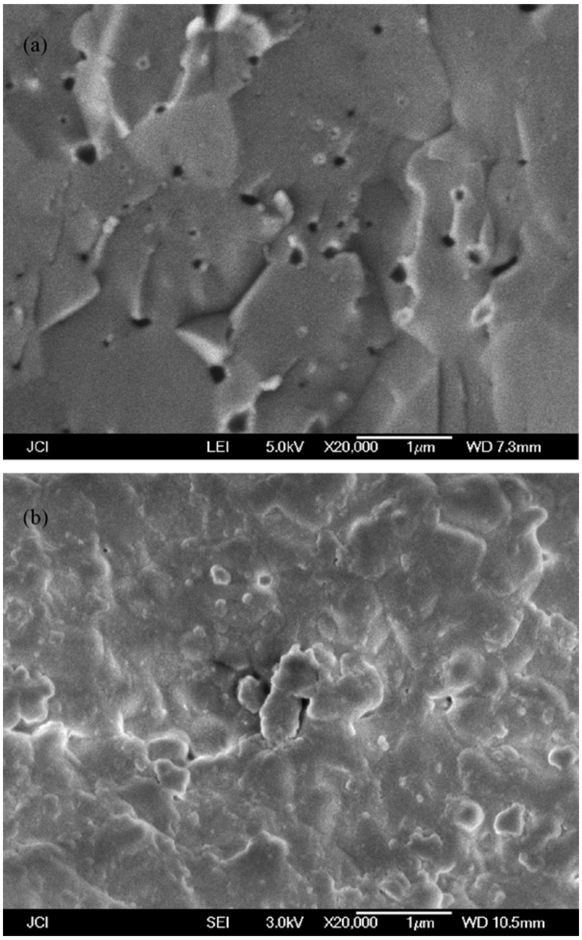

Fig. 6. Cross-section (a) and surface (b) views of a YSZ pellet.

Shown in Fig. 6 are the surface and cross-SEM images of a sintered pellet. As shown in Fig. 6, grain boundary was not clear, and average grain size was about 2 μm. In addition, the YSZ pellets had a few closed pores of about 0.1 μm in size at grain boundary or within grain body.

3.3. Electrical properties of the sintered samples

Shown in Fig. 7 are impedance spectra measured at 600 °C for pellets with different thickness. One full arc was observed at high frequency. The low frequency arc should be caused by diffusion. To verify whether or not the only full arc is associated with the electrode parameters, the pellet thickness was varied. The resistance of the electrolyte changes with the length of the specimen (D), while the resistance of the electrodes does not. As shown in Fig. 7, the values of the resistance determined by the difference between the intercepts of the full arcs with the real axis change with the thickness. The resistance is 8.0 Ω for $D = 0.58$ mm and 17.5 Ω for $D' = 1.10$ mm. Therefore, the resistance changes with the thickness and is in proportion to the thickness. From these considerations it is concluded that the full arcs in Fig. 7 represents the response of the electrolytic resistance not the electrode. A better characterization of electrical transport in ceramics can be achieved by impedance spectroscopy because with this technique it may be possible to separate bulk and grain boundary contributions, porosity, and second phase blocking effects, as well as electrode processes [1]. He et al. [13] pointed out the left side intercept of the impedance arcs with the abscissa axis is a measurement of the grain resistance, and the right side intercept of the impedance arcs with the abscissa axis is corresponding to grain and grain-boundary resistances. This is consistent with our result. Brune [1] has also shown the grain boundary and bulk contributions could be resolved as separated arcs for YSZ prepared by a co-precipitating method. As shown in Fig. 7, the grain and grain-boundary resistances are clearly separated when YSZ is prepared with the glycine-nitrate process. Our results further show that conductivities at low temperature were limited by grain-boundary resistances, and these at high temperature were controlled by grain resistances. At 500 °C, for example, the grain resistance possessed 33% of the total resistance for 120-YSZ while it was 38% for 70-YSZ. This also suggests that the amount of glycine has an effect on grain boundary and bulk contributions.

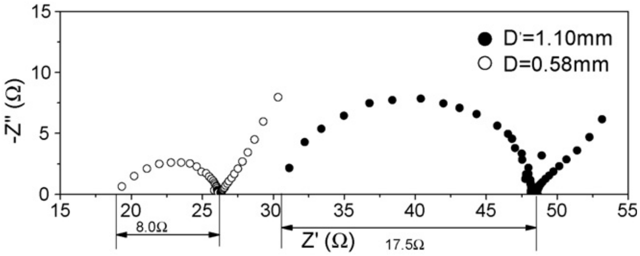

Fig. 7. Variation in the impedance spectra with the sample thickness.

Fig. 8 presents the plots for conductivity of 70-YSZ and 100-YSZ. The conductivities at 800 °C of the other samples are listed in Table 1. The conductivities of 70-YSZ and 80-YSZ pellets are bigger than those of the others. It is possibly caused by the relatively high sinterability of the 70-YSZ and 80-YSZ powders. For the conductivity dominated by grains, the following relationship has been given [13]: $R_g = \rho_g(L/S)(I/\rho_{th})$, where R_g is the total grain resistance, ρ_g the resistivity of the grains, L the thickness of the samples, S the electrode area,

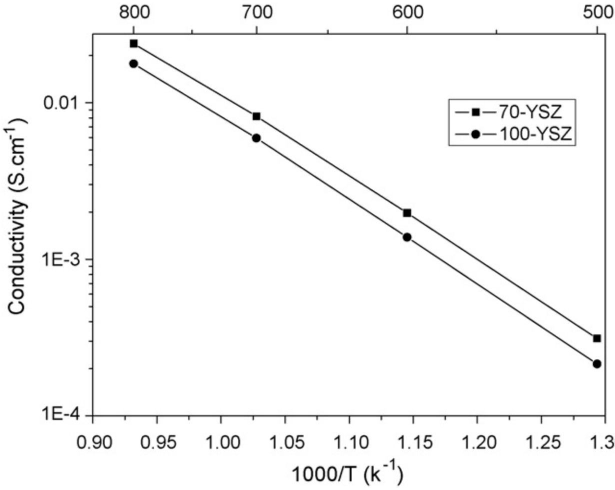

Fig. 8. The total conductivity vs. the amount of glycine.

and ρ_{th} is the relative density. So total grain resistance R_g is inversely proportional to ρ_{th}. That is, the higher the relative density, the smaller the total grain resistance, and the larger the grain conductivity, which suggested that the relative density of the specimen seems to be responsible for the difference between the conductivities. It should be noted that the relative density is not the only factor affecting the conductivity. The factors affecting conductivity include not only measured temperature and atmosphere, but also powder characteristic, relative density, the degree of association among point defects, the occurrence of order–disorder transition and the equilibration of the YSZ with oxygen during annealing.

4. Conclusions

With glycine-nitrate process, finely dispersed and weakly agglomerated nanocrystalline YSZ with the average crystallite size of 8 nm was synthesized when the powders was fired at 600 °C. YSZ powders were prepared with glycine from 70% to 120% of stoichiometric amount. These powders exhibited a cubic structure when fired at temperature above 600 °C. And their crystallite size increased with the amount of glycine and heating temperature. The flame temperature of the glycine-nitrate combustion reaction increased with glycine quantity. High temperature leads to further crystalline growth, thus low specific surface area. In addition, the morphology and sinterability of YSZ particle were affected by the glycine quantity. Powders prepared with low glycine quantity are much easy to be densified. As a result, YSZ prepared with these powders had high conductivity. The highest conductivity was 0.027 S cm^{-1} at 800 °C when YSZ was fired at 1400 °C for 5 h. YSZ prepared by the glycine-nitrate process as described above can find applications in preparing dense YSZ film with a dry-press technique, where very low packing density is beneficial.

Acknowledgements

This work was supported by the Natural Science Foundation of China (50332040 and 50372066) and also by the China Ministry of Education (SRFDP20050358023). H.W. thanks the Australian Research Council for the QEII Fellowship.

References

[1] A. Brune, M. Lajavardi, D. Fisler, J.B. Wagner Jr., Solid State Ionics 106 (1998) 89–101.

[2] A. Weber, E. Ivers-Tiffee, J. Powder Sources 127 (2004) 273–283.

[3] P. Lenonrmand, D. Caravaca, C. Laberty-Robert, F. Ansart, J. Eur. Ceram. Soc. 25 (2005) 2643–2646.

[4] S.P.S. Badwal, F.T. Ciacchi, Adv. Mater. 13 (12/13) (2001) 993–996.

[5] I.R. Gibson, G.P. Dransheld, J.T.S. Irvine, J. Mater. Sci. 33 (1998) 4297–4305.

[6] A. Diaz-Parralejo, A. Macias-Garcia, E.M. Cuerda-Correa, J. Non-Cryst. Solids 351 (24–26) (2005) 2115–2121.

[7] X.S. Xin, Z. Lu, Z.H. Ding, X.Q. Huang, Z.G. Liu, X.Q. Sha, Y.H. Zhang, W.H. Su, J. Alloy Compd. 425 (1/2) (2006) 69–75.

[8] G. Dell'Agli, S. Esposito, G. Mascolo, J. Eur. Ceram. Soc. 25 (12) (2005) 2017–2021.

[9] C.R. Xia, M.L. Liu, J. Am. Ceram. Soc. 84 (8) (2001) 1903–1905.

[10] C.R. Xia, M.L. Liu, Solid State Ionics 144 (2001) 249–255.

[11] Z. Liu, H. Zhou, Rare Met. Mater. Eng. 34 (Suppl.) (2005) 135–137.

[12] S. Saha, S.J. Ghanawat, R.D. Purohit, J. Mater. Sci. 41 (7) (2006) 1939–1943.

[13] T.M. He, Q. He, N. Wang, J. Alloy Compd. 396 (2005) 309–315.

[14] R.R. Peng, C.R. Xia, Q.X. Fu, G.Y. Meng, D.K. Peng, Mater. Lett. 56 (2002) 1043–1047.

[15] X.S. Xin, Z. Lu, X.Q. Huang, X.Q. Sha, Y.H. Zhang, K.F. Chen, N. Ai, R.B. Zhu, W.H. Su, J. Powder Sources 160 (2006) 1221–1224.